Measurement of the $^2S_{1/2}$-$^2D_{5/2}$ clock transition in a single $^{171}Yb^+$ ion

M. Roberts,[1] P. Taylor,[1] S. V. Gateva-Kostova,[2] R. B. M. Clarke,[3] W. R. C. Rowley,[1] and P. Gill[1]
[1]*National Physical Laboratory, Queens Road, Teddington, Middlesex TW11 0LW, United Kingdom*
[2]*Institute of Electronics, Boulevard Tsarigradsko Shausse 72, 1784 Sofia, Bulgaria*
[3]*Department of Physics and Applied Physics, University of Strathclyde, 107 Rottenrow, Glasgow G4 0NG, United Kingdom*
(Received 20 November 1998)

Spectroscopy of the 411-nm transition in $^{171}Yb^+$ has been performed and the feasibility of its use as an optical frequency standard has been demonstrated. The $^2S_{1/2}(F=0,\ m_F=0)-^2D_{5/2}(F=2,\ m_F=0)$ frequency, at zero-magnetic field, has been measured to be 729 487 779 566(153) kHz. This transition is free from the first-order Zeeman shift and has a measured second-order shift of $+0.38(8)$ Hz/$(\mu T)^2$. In addition, the hyperfine structure of the $^2D_{5/2}$ level has been deduced by driving the other hyperfine components of the 411-nm transition, showing it to be inverted. The $^2D_{5/2}$ hyperfine splitting, measured to be $-191(2)$ MHz, implies an A factor of $-63.6(7)$ MHz. These data taken in conjunction with previous work yield an isotope shift of $\nu_{171}-\nu_{172}=+1317.1(1.3)$ MHz for this transition between the 171 and 172 isotopes.
[S1050-2947(99)08110-X]

PACS number(s): 32.10.Fn, 06.30.Ft, 32.80.Pj, 42.50.Lc

I. INTRODUCTION

The construction of a reproducible frequency standard depends critically on the ability to control perturbations to the reference system. A single ion, stored in an electrodynamic (Paul) trap, is particularly suitable as a reference since perturbations can be effectively controlled. The quantum-jump technique [1] can be used to observe a narrow forbidden transition, which is an excellent reference for a high-stability frequency standard. Tight confinement of the ion in the Lamb-Dicke regime [2] eliminates the first-order Doppler effect and recoil shift. The second-order Doppler shift can be reduced by laser cooling the ion and by careful control of the ion's motion. Operation under ultrahigh-vacuum conditions reduces pressure shifts to a negligible level and the use of a single particle eradicates collective effects.

The choice of atom is critical if a standard with the best possible reproducibility is to be constructed. Insensitivity to magnetic fields and consequent improvement in reproducibility is provided by using an $m_F=0$-$m_F=0$ transition in an atom with integer total angular momentum. Many isotopes of various atoms have this property, but to make laser cooling and state preparation simple, it is desirable to use an alkali-like ion with a nuclear spin of $\frac{1}{2}$. The only species currently under investigation, which meet all of these criteria, are $^{199}Hg^+$ and $^{17}Yb^+$.

The ytterbium ion has several transitions that are suitable as optical-frequency references, all of which are being actively investigated: the ultranarrow 467-nm $^2S_{1/2}$-$^2F_{7/2}$ transition [3], the 435-nm $^2S_{1/2}$-$^2D_{3/2}$ transition [4], the 411-nm $^2S_{1/2}$-$^2D_{5/2}$ transition [5] (this paper), and the infrared $^2F_{7/2}$-$^2D_{5/2}$ 3.43-μm transition [6]. To the best of our knowledge, this paper is the first study of the 411-nm $^2S_{1/2}$-$^2D_{5/2}$ transition in the 171 isotope. The $^2D_{5/2}$ level has a lifetime of 7.2(3) ms [5] giving the 411-nm transition a Q of 3×10^{13}, making it acceptable as a high-stability frequency reference. The previous work on this transition [5] has used the technically easier 172 isotope. Due to the absence of hyperfine structure, it is easier to perform spectroscopy in the 172 isotope; however, the lack of $m_F=0$-$m_F=0$ transitions make the 172 isotope unsuitable for use as a frequency standard.

The first part of this paper describes laser cooling the 171 isotope. The next section describes investigation of the 411-nm clock transition and its hyperfine structure. Following this is a measurement of the second-order Zeeman shift and an absolute frequency measurement of the $F=0$-$F=2$ component of the $^2S_{1/2}$-$^2D_{5/2}$ transition. Finally, a measurement of hyperfine splitting of the $^2D_{5/2}$ level is described, and the isotope shift of the 411-nm transition between the 171 and 172 isotopes is deduced.

II. COOLING THE 171 ISOTOPE OF YTTERBIUM

A single ion of $^{171}Yb^+$ is confined in a Paul trap consisting of a ring and two endcap electrodes. An ac voltage is applied to the ring to form a pseudopotential well in which the ion is confined. In addition a dc voltage is applied to the ring to equalize the axial and radial oscillation frequencies $\omega_r\approx\omega_z\approx2\pi\times1.1$ MHz. The rf-photon correlation technique [7] is used to minimize the micromotion in the direction of the cooling laser beam. The background pressure in the trap is less than 10^{-10} mbar, and ion storage times of over one month have been observed.

The levels involved in the laser-cooling scheme are shown in Fig. 1. The 171 isotope of Yb^+ has a spin of $\frac{1}{2}$, which causes hyperfine doublets in the energy-level structure. Laser cooling of this isotope of ytterbium has been performed by several groups (e.g., [8–10]). In this paper the single ion is laser cooled by repeatedly driving the $F=1$-$F=0$ component of the $^2S_{1/2}$-$^2P_{1/2}$ transition with laser radiation at 369 nm. From the $^2P_{1/2}(F=0)$ state there is a small probability for decay into the metastable $^2D_{3/2}(F=1)$ state. To maintain the cooling cycle, the $^2D_{3/2}$ level is rapidly depopulated by a laser at 935 nm, returning the ion to the $F=1$ ground state via the $^3D[3/2]_{1/2}(F=0)$ level. The 369-nm laser wavelength in the 171 isotope was deduced using the isotope shift data of Mårtensson-Pendrill, Gough, and Hannaford [11], and the necessary 935-nm wavelength from the work of Tamm, Schnier, and Bauch [12]. This cool-

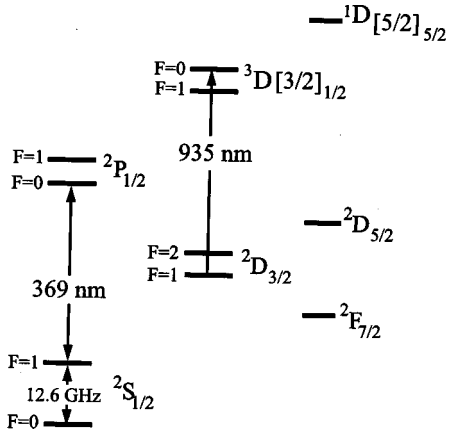

FIG. 1. Partial term scheme of $^{171}Yb^+$ showing the levels and transitions involved in the laser cooling cycle.

ing cycle forms a closed loop, but nonresonant excitation of the $^2P_{1/2}(F=1)$ state by the cooling laser leads to optical pumping of the $F=0$ ground state. In order to achieve effective cooling, the $F=0$ ground state must be coupled to the cooling cycle. In this paper this is done by driving the $F=0$-$F=1$ ground-state transition with microwave radiation at 12.6 GHz. The microwave radiation is generated by an HP3732B frequency synthesizer, amplified to obtain 1-W output power, and applied to one of the pins of the vacuum feedthrough close to the ring electrode. No special precautions are taken to ensure impedance matching. This microwave transition is also being investigated by many groups as a frequency standard in its own right [9,12–14]. To date, the best measurement of the transition frequency is 12 642 812 118.466(2) Hz [13].

In zero magnetic field no fluorescence is observed from the cooling transition. This is due to coherent population trapping in the $m_F=\pm 1$ sublevels of the $F=1$ ground state. The rate of depopulation as a function of the magnetic field is governed by the Lamor frequency, $\omega_L=g_F\mu_B B/\hbar$. The rate of population, with the cooling laser driven at saturation, is governed by the lifetime of the $^2P_{1/2}$ level τ, which is 8.1 ns [15,16]. Achieving effective depopulation, and hence seeing adequate fluorescence, requires that $\omega_L \gtrsim 1/\tau$, i.e., $B \gtrsim \hbar/g_F\mu_B\tau$. A plot of fluorescence verses magnetic field gives a Lorentzian-shaped dip, with a half width of 300 μT, in reasonable agreement with this crude theory. It is also important to choose the magnetic-field direction, relative to the cooling-laser polarization, such that both $\Delta m_F=0$ and ± 1 transitions are driven. It was found that above a magnetic field of 1 mT, applied at 45° to the cooling-laser polarization, no increase in fluorescence was observed. This magnetic field is almost two orders of magnitude larger than that required for the 172 isotope. In the even isotope coherent population trapping occurs only in the $^2D_{3/2}$ level, which is populated much less frequently than the ground state because of the small $^2P_{1/2}$-$^2D_{3/2}$ branching ratio. Another technique for avoiding population trapping in the cooling transition is to ''spin'' the polarization of the cooling laser [17], which is advantageous since it avoids the use of a large magnetic field.

Figure 2 shows a fluorescence profile of a single $^{171}Yb^+$ ion as the frequency of the cooling laser is scanned over the

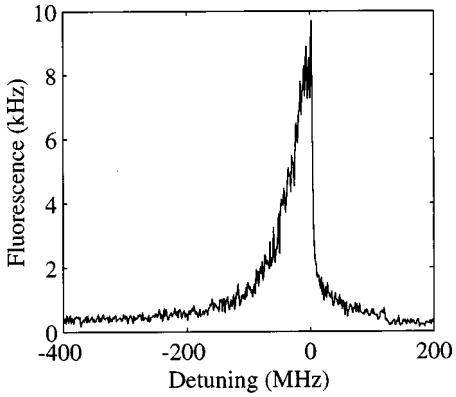

FIG. 2. Profile of the cooling transition.

$^2S_{1/2}$-$^2P_{1/2}$ resonance. A characteristic asymmetric line shape is observed due to the heating of the ion at frequencies greater than line center. A maximum count rate of 12 kHz has been obtained, compared with a typical $^{172}Yb^+$ count rate of 35 kHz. Driving the ground-state hyperfine transition halves the population in the cooling cycle, and so halves the maximum possible fluorescence. A more effective, but nontrivial scheme, would be to depopulate the $F=0$ ground state by placing a frequency sideband on the 369-nm light [4], thus also driving the $F=0$-$F=1$ transition. The remainder of the missing fluorescence is most likely due to inefficient depopulation of the $^2D_{3/2}(F=2)$ level by nonresonant 935-nm radiation. This could be avoided by a second 935-nm repumping laser, or switching the laser frequency between the two transitions.

III. SPECTROSCOPY OF THE $^2S_{1/2}$-$^2D_{5/2}$ TRANSITION

The term scheme relevant to the clock cycle is shown in Fig. 3. The electric quadrupole $^2S_{1/2}$-$^2D_{5/2}$ transition at 411 nm is investigated using the quantum-jump technique. From the $^2D_{5/2}$ level the ion can decay either to the $^2F_{7/2}$ level via an electric dipole transition, or back to the ground state. The branching ratio for decay to the $^2F_{7/2}$ level has been measured [5] in $^{172}Yb^+$ as 0.83 ± 0.03. Due to the ten-year lifetime of the $^2F_{7/2}$ level it is necessary to depopulate this state by driving an additional transition. As in previous work [5] the electric quadrupole $^2F_{7/2}$-$^1D[5/2]_{5/2}$ transition at 638 nm is used for this purpose. The work presented here shows that the hyperfine structure of the $^2D_{5/2}$ level is inverted. From the present paper it is not possible to determine whether the $^2F_{7/2}$ or $^1D[5/2]_{5/2}$ levels are inverted.

Figure 4 shows a schematic of the experimental arrangement. A single ion is tightly confined in the trap where it is laser cooled close to the Doppler limit. The resonance fluorescence at 369 nm is detected by the photomultiplier. This fluorescence is used to monitor the state of the ion. The cooling laser and microwave radiation are chopped in antiphase with the 411-nm laser to avoid broadening the ground-state transition during the probe interrogation. Laser light at 411 nm is used to drive the $^2S_{1/2}$-$^2D_{5/2}$ transition, producing a quantum ''off'' jump. The long-lived $^2F_{7/2}$ state is depopulated by light from an extended cavity diode laser at 638 nm, producing a quantum ''on'' jump. The 638-nm light is gated by an acousto-optic modulator (AOM) and only

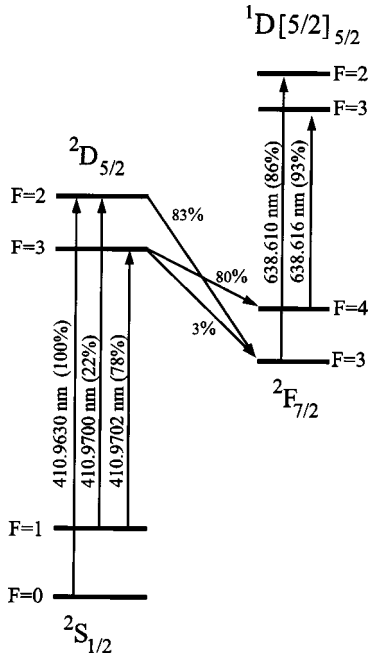

FIG. 3. Partial term scheme of $^{171}Yb^+$ showing the transitions involved in the clock-interrogation cycle. Vacuum wavelengths are given for each transition. The percentages in brackets are the calculated absorption probabilities for an ion in that particular hyperfine level [20]. The two weak $^2F_{7/2}$-$^1D[5/2]_{5/2}$ transitions (7%, 14%) are not shown. The three percentages without brackets are the branching ratios for decay from the $^2D_{5/2}$ level [20,5]. For clarity the $^2D_{5/2}$-$^2S_{1/2}$ decays are not shown.

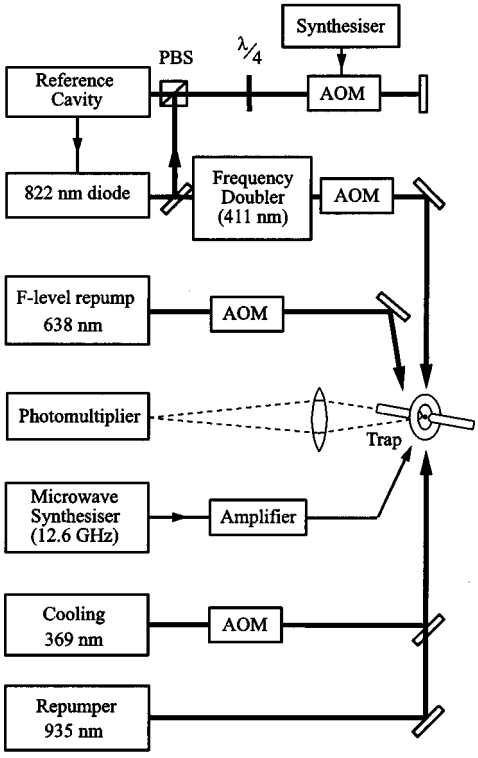

FIG. 4. Experimental arrangement. AOM—acousto-optic modulator. PBS—polarizing beam splitter.

illuminates the ion when the fluorescence has remained ''off'' for an appropriately long time, indicating that the ion is in the $^2F_{7/2}$ state. The data acquisition program switches the AOMs in sequence and records the fluorescence level. To obtain a transition profile of a particular 411-nm hyperfine component, the 411-nm laser frequency is stepped over the transition by the synthesizer-controlled AOM. A histogram of quantum-jump statistics is produced. A number of these scans is taken and the data from them summed to produce a profile with satisfactory statistics. In order to observe all of the Zeeman components the 1 mT magnetic field is applied at roughly 45° to both the 411-nm laser polarization and the direction of propagation.

Collisions with background gas can cause a transition from the $^2D_{3/2}$ to the $^2F_{7/2}$ level. The resulting event is indistinguishable from a quantum jump caused by the 411-nm laser and hence forms a background to the experiment. In the current experiment the laser-frequency-independent background was less than one jump per hour. Each data set consists of around 300 jumps taken over a period of around one hour; hence, the pressure-induced jumps are statistically insignificant.

Light at 411 nm is generated using a frequency-doubled diode laser [8]. The frequency of the laser is stabilized to a Fabry-Perot reference cavity, which is mounted in an evacuated, temperature-controlled chamber. The cavity, made from optically contacted ultralow-expansivity material has a transmission linewidth of approximately 1 MHz at 822 nm. The Pound-Drever-Hall technique is used to stabilize the laser to the cavity resonance, using frequency-modulated sidebands placed on the laser light at 10 MHz by direct modulation of the laser-diode current. Feedback is applied to the extended-cavity grating and diode-injection current. Frequency scanning of the laser is provided by a double-passed AOM between the laser and reference cavity. The AOM is capable of scanning from 180–380 MHz. The drive frequency of the AOM is produced by a frequency synthesizer, which is controlled by the data-acquisition program. The 822-nm light is frequency doubled to 411 nm in a critically phase-matched crystal of lithium triborate. The crystal is located at the tight focus of an enhancement cavity for the fundamental light. This frequency doubling scheme has been described previously [5], except that in this paper the enhancement cavity is kept in resonance with the 822-nm radiation by the Hänsch-Couillard technique [18].

The 638-nm laser depopulates the $^2F_{7/2}$ state via the high-lying $^1D[5/2]_{5/2}$ level. The $^1D[5/2]_{5/2}$ level decays to the cooling cycle via either the $^2D_{3/2}$ or the $^2D_{5/2}$ level. The 638-nm laser frequency is switched [19] by a few gigahertz so that both the $F=3$ and $F=4$ hyperfine states of the $^2F_{7/2}$ level are depopulated, and it is frequency dithered by several megahertz so that all of the Zeeman components of the transition are encompassed. Figure 3 shows the relationship between the 411-nm transitions and the 638-nm transitions used to depopulate the $^2F_{7/2}$ level. The percentages in brackets show the calculated relative absorption probabilities [20] for an ion in that particular hyperfine level. As the levels are selectively populated by a single ion and not by an ensemble, no statistical weighting factors are required. Only two of the four possible 638-nm transitions have been observed. This is due to the large differences in relative intensities of the tran-

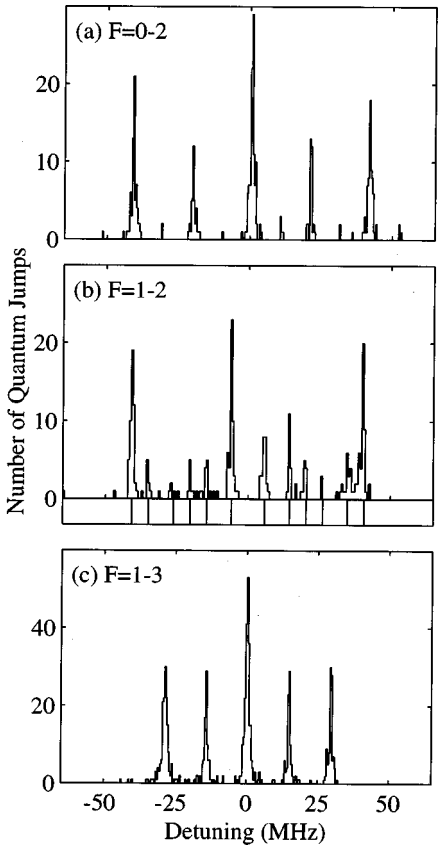

FIG. 5. Zeeman structure of the 411-nm $^2S_{1/2}$-$^2D_{5/2}$ transition. (a) $F=0$-$F=2$, (b) $F=1$-$F=2$, and (c) $F=1$-$F=3$. To aid the eye, (b) shows the expected positions of the Zeeman components below the picture.

sitions. It was possible to identify the levels involved in the various 411-nm transitions by the strong dependence on which 638-nm transition was necessary to depopulate the $^2F_{7/2}$ level. These assignments were later confirmed by a detailed examination of the Zeeman structure of the 411-nm transition.

The Zeeman structures of the three 411-nm transitions are shown in Fig. 5. Figure 5(a) shows the $F=0$ to $F'=2$ transition. In this picture the Zeeman structure is fully resolved. The small amount of background between the main peaks are micromotion sidebands. A measurement of the frequency of the central component ($m_F=0$ to $m_F'=0$) is described in a later section. The relative intensities of the Zeeman components are in good agreement with theory for this hyperfine component. Figures 5(b) and 5(c) show the $F=1$ to $F'=2$ and 3 transitions. The calculated relative absorption strengths of the hyperfine transitions (Fig. 3) agree qualitatively with the observed strengths (i.e., $F=1$ to $F'=2$ is weaker than $F=1$ to $F'=3$). The Zeeman structure of the $F=1$ to $F'=2$ transition has 12 unevenly spaced components, which are resolved in the picture. As expected, the $m_F=0$ to $m_F'=0$ component is absent, being forbidden on angular momentum grounds. The weakness of the $F=1$ to $F'=2$ transition is responsible for the comparatively poor statistics in the figure, which makes the weakest pair of Zeeman components barely observable. Despite this it is quite clear that the relative intensities of the various components are not symmetric about zero detuning. This is caused by an imbalance

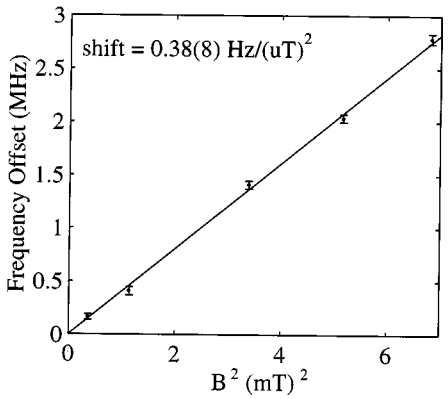

FIG. 6. Second-order Zeeman shift of the $^2S_{1/2}(F=0,\ m_F=0)$-$^2D_{5/2}(F=2,\ m_F=0)$ transition.

in the populations of the ground-state sublevels, which is induced by the cooling radiation [21]. The $F=1$ to $F'=3$ transition in Fig. 5(c) consists of 15 Zeeman components. Each observed peak consists of three unresolved Zeeman transitions. This is due to the g_F factors of the $^2S_{1/2}(F=1)$ and $^2D_{5/2}(F'=3)$ hyperfine levels being 0.999 and 1.002, respectively. Careful analysis of the relative intensities of the Zeeman components reveals a small amount of asymmetry, again due to an imbalance in the population of ground-state sublevels. The Zeeman splittings of all of the components in all three transitions are in good agreement with theory.

IV. SECOND-ORDER ZEEMAN EFFECT

The $^2S_{1/2}(F=0)$-$^2D_{5/2}(F=2,\ m_F=0)$ transition is suitable as a frequency reference as it is free from the linear Zeeman effect. However, it is susceptible to the second-order Zeeman effect. This shift is small, but can be observed when large magnetic fields are applied to the ion. To obtain an unperturbed value for the frequency of this transition it was necessary to measure the second-order Zeeman effect and then correct it to zero field.

To deduce the unperturbed center frequency at zero applied magnetic field, a series of quantum-jump profiles were taken for various applied magnetic fields. The magnetic field was generated by three pairs of coils situated orthogonally around the trap. The field at the ion was calculated from the dimensions of the coils, and the currents passed through them. The results of these scans are shown in Fig. 6. A linear dependence of frequency with the square of applied magnetic field is clearly seen. The second-order Zeeman shift inferred from this data is 0.38(8) Hz/(μT)^2, where the error includes the rather large uncertainty in the magnetic field.

In a frequency standard application it is desirable that the second-order Zeeman shift is small, so that the associated frequency uncertainty is also small. To achieve this it will be necessary to probe the ion in a magnetic field close to zero. To avoid significantly reducing the observed cooling fluorescence by coherent population trapping it will be necessary to either observe the ion in a large field, which is switched off for the probe interrogation, or spin the cooling laser polarization [17].

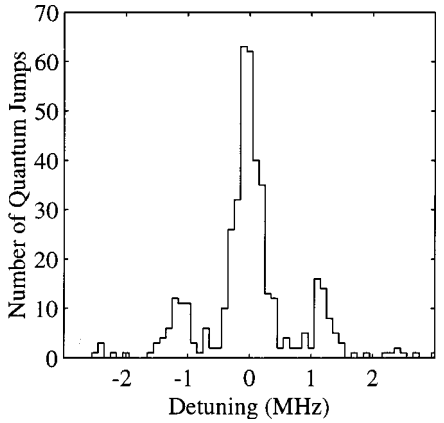

FIG. 7. Profile of the $^2S_{1/2}(F=0,\ m_F=0)$–$^2D_{5/2}(F=2,\ m_F=0)$ transition.

V. ABSOLUTE FREQUENCY MEASUREMENT

An absolute frequency measurement of the $^2S_{1/2}(F=0,\ m_F=0)$–$^2D_{5/2}(F=2,\ m_F=0)$ transition was made. The measurement consists of two parts: measuring the transmission fringe frequency of the reference cavity to which the fundamental 822-nm light was locked, and then scanning across the transition while recording the AOM frequency to obtain a quantum-jump profile of the transition. It is also necessary to take into account the frequency shift of −60.000 MHz, introduced by the AOM used to chop the 411-nm light. The data was taken in a magnetic field of 1.07(0.10) mT, and the final answer then corrected to zero field using the second-order Zeeman-shift data of the previous section. The transition was measured on two separate days. These two measurements were consistent with each other, and the final answer was obtained by combining the results of these two measurements.

To measure the reference cavity transmission fringe at 822 nm, the fundamental light was sent, by single-mode optical fiber, to the National Physical Laboratory intercomparator [22,23]. This device is a 1-m etalon that is referenced to an iodine-stabilized He-Ne, and allows wavelength comparisons with an accuracy of better than 2 parts in 10^{10}. The cavity frequency was measured before and after a series of quantum-jump scans in order to correct for any frequency drift of the reference cavity. The observed drift, of typically 200–400 kHz over several hours, is due to imperfect temperature control of the reference cavity. This drift was corrected to first-order by recording the time at which the individual scans were made, and assuming a linear drift of the cavity. An error of $0.25\times$(total drift) is allowed in this correction. The intercomparator has a number of systematic errors that amount to 30 kHz [5], and measurement statistics of 30–40 kHz. Both the cavity drift and intercomparator errors apply to the fundamental frequency of 822 nm and so are doubled to find the contribution to the measurement at 411 nm.

A typical scan of the $m_F=0$ to $m_F'=0$ component is shown in Fig. 7. The profile consists of three features. The central feature is the Doppler-free resonance of the transition, while the two smaller peaks are secular-motion sidebands. These sidebands consist of three unresolved components corresponding to the three spatial axes. The motional peaks are separated from the carrier by the secular frequency $\omega_r \approx \omega_z \approx 1.1$ MHz. From the intensities of the sidebands, it is clear that the ion is in the Lamb-Dicke regime. An ion temperature of 0.63 mK can be estimated from these intensities, which is close to the Doppler limit of 0.47 mK. The line-center frequency was determined by taking the mean of the data for the central peak only. This is to avoid line-pulling effects, which could be caused by unequal intensities of the motional sidebands. The measurement statistics on finding the line center of these profiles is only a few kilohertz, and so makes little contribution to the final error. The final value for the frequency of the transition, obtained from combining the results of the two days' measurements, is 729 487 779 566(153) kHz.

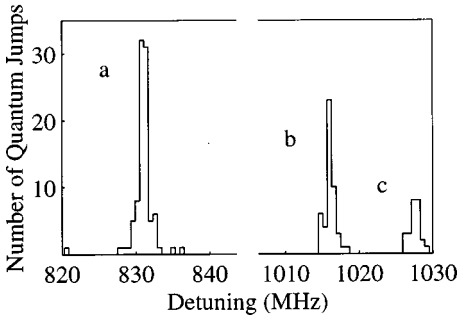

FIG. 8. Hyperfine splitting of the $^2D_{5/2}$ level. Feature *a* is the $\Delta m_F=0$ component of the $F=1$ to $F'=3$ transition. Features *b* and *c* are the $m_F=-1$ to $m_{F'}=-1$ and $m_F=+1$ to $m_F=+1$ components of the $F=1$ to $F'=2$ transition. The hyperfine splitting is the difference in frequency between component *a* and the mean of components *b* and *c*.

VI. HYPERFINE SPLITTING AND ISOTOPE SHIFT

The hyperfine splitting of the $^2D_{5/2}$ level is determined by the difference in frequency of the transitions from the $F=1$ ground state to the two $^2D_{5/2}$ hyperfine levels. It was possible to scan between these two transitions while locked to the same mode of the reference cavity, making the measurement of the splitting relatively simple. For the $F=1$ to $F'=3$ transition the central component ($\Delta m_F=0$) is measured. For the $F=1$ to $F'=2$ transition the absence of the $m_F=0$ to $m_F'=0$ component means that the line center is derived from the mean frequency of the $m_F=-1$ to $m_F'=-1$ and the $m_F=+1$ to $m_F'=+1$ transitions, which are the central two components in Fig. 5(b). The results of these scans are shown in Fig. 8. A hyperfine splitting of 190.9(0.2) MHz is calculated from this data. However, this neglects the second-order Zeeman shift. It is possible to estimate an upper limit on this shift, since a large effect would cause line asymmetry in the observed line shapes. By the absence of significant asymmetry it is possible to put an upper limit of 2 MHz on the second-order Zeeman shift. The best measure of the hyperfine splitting is, therefore, −191(2) MHz. This implies an A factor of −63.6(7) MHz. No B factor is present since the nuclear spin $I=\frac{1}{2}$.

The centroid of the 411-nm transition is calculated using the weighted splitting of the $^2S_{1/2}$ and $^2D_{5/2}$ levels, and the absolute measurement of the $F=0$-$F'=2$ transition. This centroid frequency, ν_{171}, is then used with a previous mea-

surement [5] of the 411-nm transition in the 172 isotope, ν_{172}, to give an isotope shift $\nu_{171}-\nu_{172} = +1317.1(1.3)$ MHz.

VII. CONCLUSION

Spectroscopy of the 411-nm $^2S_{1/2}(F=0)-^2D_{5/2}(F=2,\ m_F=0)$ transition has been performed and the feasibility of its use as an optical-frequency standard has been demonstrated. The center frequency at zero magnetic field has been measured to be 729 487 779 566(153) kHz. This measurement therefore has an uncertainty of 2 parts in 10^{10}. The transition is free from the first-order Zeeman shift, and the second-order shift has been measured to be 0.38(8) Hz/$(\mu\mathrm{T})^2$. As an example, to achieve a shift due to the Zeeman effect of 1 part in 10^{15} requires the residual magnetic field at the ion to be reduced to 2 μT, a level that is readily achievable. A better measurement of the magnetic field, and thus improved knowledge of the associated shift, could be obtained by measuring the $\Delta m_F=\pm 1$ components of the 411-nm transition.

In addition, the hyperfine structure of the $^2D_{5/2}$ level has been deduced by driving the other 411-nm hyperfine components, and has been shown to be inverted. The $^2D_{5/2}$ hyperfine splitting has been measured to be $-191(2)$ MHz, which implies an A factor of $-63.6(7)$ MHz. These data are used with a previous measurement [5] to give an isotope shift for the 411-nm transition of $\nu_{171}-\nu_{172}=+1317.1(1.3)$ MHz.

In addition to its use as an optical-frequency standard, the measurement of the 411-nm transition will facilitate the location of the extremely weak $^2S_{1/2}$-$^2F_{7/2}$ electric octupole transition at 467 nm. A measurement of the $^2F_{7/2}$-$^2D_{5/2}$ 3.43-μm transition will be used in conjunction with this measurement to indirectly measure the octupole transition frequency, yielding a starting point in a search for the transition. The 467-nm octupole transition is also being considered as an optical-frequency standard and has already been observed in the technically easier $^{172}Yb^+$ isotope [3]. The extremely long lifetime of the upper level of this transition make it of particular interest as an optical-frequency standard.

It should be possible to make a high-stability frequency standard based on the $^2S_{1/2}$-$^2D_{5/2}$ transition. The $^2D_{5/2}$ level lifetime [5] of 7.2 ms implies a natural linewidth of 22 Hz, and hence a line Q of 3×10^{13}. To realize the full stability of the standard it would be necessary to interrogate the transition with a sub-20-Hz linewidth laser. As an example, with a 0.7-ms interrogation time, a laser locked to this transition would have a stability [24] of $\sigma_y(\tau)=8\times10^{-15}/\sqrt{\tau}$.

The feasibility of using the $^2S_{1/2}$-$^2D_{5/2}$ transition as a frequency reference has been demonstrated. This is made possible, despite the decay of the $^2D_{5/2}$ level into the $^2F_{7/2}$ level, by switching the laser at 638 nm used to depopulate the $^2F_{7/2}$ level between two hyperfine components. The ability to drive weak transitions that are free from the linear Zeeman effect should yield single-ion frequency standards reproducible at the part in 10^{15} level in the near future.

[1] H. Dehmelt, Bull. Am. Phys. Soc. **20**, 60 (1975).
[2] R. H. Dicke, Phys. Rev. **89**, 472 (1953).
[3] M. Roberts, P. Taylor, G. P. Barwood, P. Gill, H. A. Klein, and W. R. C. Rowley, Phys. Rev. Lett. **78**, 1876 (1997).
[4] C. Tamm and D. Engelke, in *Laser Spectroscopy XIII*, edited by Z.-J. Wang, Z.-M. Zhang, and Y.-Z. Wang (World Scientific, Singapore, 1998), pp. 180–182.
[5] P. Taylor, M. Roberts, S. V. Gateva-Kostova, R. B. M. Clarke, G. P. Barwood, W. R. C. Rowley, and P. Gill, Phys. Rev. A **56**, 2699 (1997).
[6] P. Taylor, M. Roberts, G. P. Barwood, and P. Gill, Opt. Lett. **23**, 298 (1998).
[7] D. J. Berkland, J. D. Miller, J. C. Bergquist, W. M. Itano, and D. J. Wineland, J. Appl. Phys. **83**, 5025 (1998).
[8] D. Engelke and C. Tamm, Europhys. Lett. **33**, 347 (1996).
[9] V. Enders, P. Courteille, R. Huesmann, L. S. Ma, W. Neuhauser, R. Blatt, and P. E. Toschek, Europhys. Lett. **24**, 325 (1993).
[10] P. T. H. Fisk, M. A. Lawn, and C. Coles, Appl. Phys. B: Photophys. Laser Chem. **57B**, 287 (1993).
[11] A.-M. Mårtensson-Pendrill, D. S. Gough, and P. Hannaford, Phys. Rev. A **49**, 3351 (1994).
[12] C. Tamm, D. Schnier, and A. Bauch, Appl. Phys. B: Lasers Opt. **B60**, 19 (1995).
[13] P. T. H. Fisk, M. J. Sellars, M. A. Lawn, and C. Coles, IEEE Trans. Ultrason. Ferroelectr. Freq. Control **44**, 344 (1997).
[14] D. J. Seidel and L. Maleki, Phys. Rev. A **51**, R2699 (1995).
[15] R. W. Berends, E. H. Pinnington, B. Guo, and Q. Ji, J. Phys. B **26**, 701 (1993).
[16] R. M. Lowe, P. Hannaford, and A. M. Mårtensson Pendrill, Z. Phys. D **28**, 283 (1993).
[17] D. J. Berkland, J. D. Miller, J. C. Bergquist, W. M. Itano, and D. J. Wineland, Phys. Rev. Lett. **80**, 2089 (1998).
[18] T. W. Hänsch and B. Couillaud, Opt. Commun. **35**, 441 (1980).
[19] R. N. Watts and C. E. Wieman, Opt. Commun. **57**, 45 (1986).
[20] R. D. Cowan, *The Theory of Atomic Structure and Spectra* (University of California Press, Berkley, CA, 1981).
[21] G. P. Barwood, P. Gill, G. Huang, H. A. Klein, and W. R. C. Rowley, Appl. Phys. B: Lasers Opt. **B61**, 385 (1995).
[22] G. P. Barwood, W. R. C. Rowley, and P. T. Woods, Metrologia **20**, 157 (1984).
[23] G. P. Barwood, W. R. C. Rowley, P. Gill, J. L. Flowers, and B. W. Petley, Phys. Rev. A **43**, 4783 (1991).
[24] D. J. Wineland, W. M. Itano, J. C. Bergquist, J. J. Bollinger, F. Diedrich, and S. L. Gilbert, in *Proceedings of the 4th Symposium on Frequency Standards and Metrology*, edited by A. De Marchi (Springer-Verlag, Berlin, 1989), pp. 71–77.